Molecular and Cellular Endocrinology 537 (2021) 111419

Contents lists available at ScienceDirect

Molecular and Cellular Endocrinology

journal homepage: www.elsevier.com/locate/mce

Low sodium and tolvaptan have opposite effects in human small cell lung cancer cells

Giada Marroncini [a,b,1], Cecilia Anceschi [a,b,1], Laura Naldi [a,b], Benedetta Fibbi [a,b], Federica Baldanzi [a,b], Serena Martinelli [b], Simone Polvani [c], Mario Maggi [b], Alessandro Peri [a,b,*]

[a] Pituitary Diseases and Sodium Alterations Unit, AOU Careggi, 50139, Florence, Italy
[b] Endocrinology, Department of Experimental and Clinical Biomedical Sciences "Mario Serio", University of Florence, AOU Careggi, 50139, Florence, Italy
[c] Gastroenterology, Department of Experimental and Clinical Biomedical Sciences "Mario Serio", University of Florence, AOU Careggi, 50139, Florence, Italy

ARTICLE INFO

Keywords:
Hyponatraemia
SIAD
Tolvaptan
Lung cancer

ABSTRACT

Purpose: Hyponatraemia is frequently observed in cancer patients and can be due to the syndrome of inappropriate anti-diuresis (SIAD), related to ectopic vasopressin secretion, particularly in small cell lung cancer (SCLC). Hyponatraemia is associated with a worse outcome in cancer patients. The vasopressin receptor antagonist tolvaptan effectively corrects hyponatraemia secondary to SIAD and there is *in vitro* evidence that it has also an antiproliferative effect in cancer cells. The purpose of this study was i) to analyse the effect of low serum sodium concentrations ($[Na^+]$) in SCLC cells and ii) to determine whether tolvaptan counteracts tumor progression.
Methods: We evaluated cell proliferation, cell cycle, apoptosis, oxidative stress, invasivity in low $[Na^+]$ as well as after exposure to tolvaptan. We also analysed the intracellular signalling pathways involved.
Results: In reduced $[Na^+]$ cell proliferation was significantly increased compared to normal $[Na^+]$ and cells were mostly distributed in the G2/M phase. Apoptosis appeared reduced. In addition, the ability to cross matrigel-coated membranes markedly increased. As observed in other cancer cell models, the expression of the heme-oxigenase-1 gene was increased. Finally, we found that in cells cultured in low $[Na^+]$ the RhoA/ROCK1/2 pathway, which is involved in the regulation of actin cytoskeleton, was activated. On the other hand, we found that tolvaptan effectively inhibited cell proliferation, anchorage-independent growth, invasivity and promoted apoptosis. Accordingly, the RhoA/ROCK-1/2 pathway was inhibited.
Conclusions: These findings demonstrate for the first time that low $[Na^+]$ favours tumor progression in SCLC cells, whereas tolvaptan effectively inhibits cell proliferation, survival and invasivity.

1. Introduction

Hyponatraemia, defined by a serum sodium concentration ($[Na^+]$) <135 mEq/L, is the most frequent electrolyte imbalance in cancer patients, affecting up to 40% of them at admission in Oncology Units (Doshi et al., 2012; Berardi, Rinaldi, et al., 2016). In this setting, the pathogenesis of hyponatraemia is often multifactorial, with the syndrome of inappropriate antidiuresis (SIAD) representing the leading aetiology (Grohé, 2019). The reduction of serum $[Na^+]$ secondary to SIAD is determined mainly by tumoral, ectopic secretion of arginine vasopressin (AVP) (Sørensen et al., 1995). In addition, several classes of drugs can affect the hydro-electrolytic homeostasis by stimulating AVP secretion or increasing the sensitivity of AVP-V_2 receptors expressed in renal collecting duct cells. Hence, antidepressants, analgesics (especially opioids), anticancer treatments (chemotherapeutic agents, molecular targeted agents and immune checkpoint inhibitors) and palliative medications may contribute, possibly in association with underlying conditions (e.g., intravenous hydration during chemotherapy sessions, pain and nausea), to the onset of hyponatraemia (Berardi et al., 2016b; Oronsky et al., 2017; Sørensen et al., 1995; Wanchoo et al., 2017). Among tumors that can secrete AVP, the strongest association is with lung tumors, both small cell (SCLC) and non-small cell lung cancers (NSCLC), with a prevalence of 76% (Castillo et al., 2016).

In the last decade, hyponatraemia emerged as an indicator of higher

* Corresponding author. Department of Experimental and Clinical Biomedical Sciences "Mario Serio", University of Florence, AOU Careggi, Viale Pieraccini, 6, 50139, Florence, Italy.
E-mail address: alessandro.peri@unifi.it (A. Peri).
[1] these authors equally contributed.

https://doi.org/10.1016/j.mce.2021.111419
Received 22 April 2021; Received in revised form 27 July 2021; Accepted 7 August 2021
Available online 10 August 2021

disease burden, more compromised general status with increased length of hospital stay and health costs (Sengupta et al., 2013; Berardi, Caramanti et al., 2015; Wald et al., 2010; Berardi et al., 2019; Corona et al., 2016), poor prognosis and decreased progression-free and overall survival in patients with different malignancies (Doshi et al., 2012; Berardi et al., 2019; Hansen et al. 2010; Kim et al., 2007; Corona et al., 2013; Holland-Bill et al., 2015; Tiseo et al., 2014; Kobayashi et al., 2014; Berardi, Caramanti et al., 2015; Jeppesen et al., 2010; Farid and Prasad 2015; Fucà et al., 2019). On the other hand, the normalization of low serum [Na^+] is able to favourably affect the clinical outcome, prevent clinical complications and reduce mortality (Corona et al., 2015), even in patients with advanced tumor disease (Balachandran et al., 2015; Petereit et al., 2011). Therefore, hyponatraemia represents a negative independent prognostic factor in the oncologic setting, and its use as a biomarker to identify high-risk patients affected by lung cancer has been proposed (Kasi, 2012). In this view, the assessment of serum [Na^+] could improve the prognostic stratification of cancer patients and could be exploited to design integrated prognostic tools (Fucà et al., 2019).

To date, it has not been fully elucidated whether hyponatraemia should be considered a surrogate marker of disease severity or an independent detrimental factor directly contributing to cancer progression (Chawla et al., 2011). In order to clarify this issue, we have recently demonstrated for the first time that the reduction of extracellular [Na^+] alters *in vitro* the homeostasis of different human cancer cell lines, by promoting cell proliferation, invasion and tumorigenicity, through the induction of oxidative stress and the up-regulation of RhoA/ROCK-associated signalling (Marroncini et al., 2020).

Vaptans represent a new class of drugs developed for the treatment of euvolemic or hypervolemic hyponatraemia. These drugs are nonpeptide vasopressin receptors antagonists that bind V_2 receptors expressed in renal collecting duct cells, thus inducing water diuresis and ultimately increasing serum [Na^+]. Tolvaptan has been approved in 2009 in the U. S. and in Europe for the treatment of adult patients with hyponatraemia secondary to SIAD and in the last decade has proven to be an effective and safe pharmacological tool (Berl et al., 2010; Bhandari et al., 2017; Greenberg et al., 2015; Peri, 2013; Schrier et al., 2006). In addition to its effect on the correction of hyponatraemia, tolvaptan has shown the ability to reduce cAMP levels in kidney epithelial cells and to slow cysts formation in animal models of polycistic kidney disease (PKD) (Gattone et al., 2003; Torres et al., 2004; Wang et al., 2006). Interestingly, tolvaptan has been also approved for the treatment of autosomal dominant PKD and its efficacy in reducing renal cyst growth and the estimated glomerular filtration rate (eGFR) decrease in patients has been demonstrated (Torres et al, 2012, 2017). As per tumoral cells, tolvaptan effectively reduced proliferation and triggered apoptosis in hepatocellular and renal carcinoma cells (Sinha et al., 2020; Wu et al., 2015).

The aims of this study were to determine i) whether low [Na^+] increases growth, survival and invasivity of SCLC cells and, if so, to investigate on the involved intracellular pathways; and ii) whether tolvaptan counteracts tumor progression in these cells.

2. Materials and methods

2.1. Chemicals and reagents

NCI-H69 human cell line (91091802), gelatin, Noble Agar, RPMI culture medium, Fetal Bovine Serum (FBS), L-glutamine and antibiotics (penicillin and streptomycin), Hank's BSS, dimethyl sulfoxide (DMSO), Tri Reagent, WST-8 (2-(2-methoxy-4-nitrophenyl)-3-(4-nitrophenyl)-5-(2,4-disulfophenyl)-2H-tetrazolium, monosodium salt) and menadione (Vitamin K3), which is a synthetic analogue of 1,4-naphthoquinone and has been used for the generation of reactive oxygen species (ROS), were purchased from Sigma Aldrich SRL (Milan, Italy). Tolvaptan powderwas kindly provided by Otsuka Pharmaceuticals and it was dissolved in DMSO to a final concentration of 10 mM.

2.2. Cell cultures

H69 cells were cultured in RPMI-1640 medium supplemented with 10% fetal bovine serum, L-glutamine and antibiotics (50U/mL penicillin and 50 μg/mL streptomycin) and maintained at 37 °C in a humidified atmosphere (5% CO2/95% air). To test the effects of low extracellular [Na^+], we used a special 2X DMEM sodium free medium (PAA M-medical, Milan, Italy), prepared as described previously (Marroncini et al., 2020). To reach the desired [Na^+], the appropriate amount of NaCl was added to media and three concentrations were obtained: 127, 115 and 90 mM. In the experimental protocol, extracellular [Na^+] was progressively lowered by daily medium changes, in order to adapt cells to target [Na^+] variations. Osmolality was maintained constant (307.8 mOsm/Kg), by adding appropriate amounts of mannitol to the standard medium, as described previously (Barsony et al., 2011; Marroncini et al., 2020). Then, cells were cultured at the target [Na^+] at 37 °C for 7 days before experiments were performed. In the second part of the study, H69 cells were cultured with RPMI medium and were treated with tolvaptan for 24, 48 and 72 h before experiments were performed.

2.3. Analysis of cell proliferation and viability

After 7 days of growth in the selected medium, cells were harvested and 10.000 cells/well were seeded in 96 well plates and treated with WST-8, which is bio-reduced by cellular dehydrogenases to an orange formazan product that is soluble in tissue culture medium and directly proportional to the number of metabolically active cells. The experiments were run according to manufacturer's protocol, and luminescence at 450 nm was recorded with a Wallac multiplate reader (PerkinElmer, Monza, Italy). The experiments were performed in eight wells/sample and at least twice.

2.4. Determination of the IC50 of tolvaptan on cell growth

Likewise, WST-8 assay was performed after treating H69 cells with increasing doses of tolvaptan (0 μM, 20 μM, 40 μM, 50μ M, 70 μM, 100 μM) for 24, 48 and 72 h, in order to find IC50. Treated cells and control cells were fed with complete culture medium containing 0.1% (v/v) DMSO, which had no effect on cell growth. The IC50 values were obtained from the cell growth curves, using GraphPad Prism 5.0 (GraphPad Software Inc., La Jolla, CA) and triplicate analyses were performed.

2.5. Cell cycle and annexin V/PI analyses

After 7 days of growth in the selected medium, H69 cells were harvested and washed twice with sterile PBS to perform Cell Cycle and annexin V/PI Assay. In order to perform cell cycle analysis, H69 cells must be fixed using 70% ethanol and stored at −20 °C for at least 3 h. Successively, 1×10^6 and 25×10^4 H69 cells were stained with 200 μl and 100 μl of Muse™ Cell Cycle and Annexin V & Dead Cell Reagent (Luminex Technology, Austin, TX, USA), respectively and samples were incubated for 30 min at room temperature and covered from light. Finally, sample were analysed with the cytofluorimeter Guava® Muse® Cell Analyser (Luminex Technology, Austin, TX, USA). Results of cell cycle analysis were expressed as % of cells in G0/G1, G2 and M phase and results of annexinV/PI were expressed as % of total apoptotic and live cells, normalized versus the control [Na^+] of 153 mM. The same procedure was performed after treating H69 cells with different concentrations of tolvaptan for 48 h and results were normalized versus control cells.

2.6. Invasion assay

Invasive migration was assessed by a standard Transwell invasion system using polycarbonate filter inserts (8 μm pore size) (Corning, New York, USA), which were coated with BD Matrigel Basement Membrane

(BD Becton, Dickinson and Company, New Jersey, USA) 0.3% for at least 1 h at 37 °C. The upper chambers were seeded with 1×10^6 H69 cells for 100 μl of serum free media and in the lower chamber FBS was added to the media, as chemoattractant. The invasion assay was developed for 24 h at 37 °C and then cells migrated into the lower side of the insert were stained with crystal violet in 0.1% methanol and were observed under the microscope. To obtain a quantitative analysis of migrated cells, the inserts were decoloured with DMSO and the dye mixture was measured by spectrophotometer (PerkinElmer, Monza, Italy) at the optical density (OD) of 560 nm.

2.7. Zimography assay

Samples for analysis were obtained from the medium supernatant. Samples were centrifuged for 10 min at 10,000×*g* at 4 °C and, to 45 μl of each one 5 μl of sample buffer (pH 6.8) was added. Sample buffer contained 100 mM Tris–HCl, 4% sodium dodecyl sulphate (SDS), 20% glycerol and 0.004% bromophenol blue. Protein molecular weight standards (Sigma Aldrich, Milan, Italy) and samples were electrophoretically separated with Protean II system (Bio-Rad, Hercules, CA), in SDS-PAGE Tris–glycine 8.0% polyacrylamide gel containing 2 mg/ml of gelatine at a constant current of 90 mV. The gels were washed twice in 2.5% Triton X-100 for 15 min to remove SDS and incubated in a rocking platform with reaction buffer (50 mM Tris–HCl, pH 7.5, 5 mM CaCl2, 200 mM NaCl and 1% Triton X-100) overnight at 37 °C. The gels were then stained with 0.1% Coomassie blue R-250 (Amersham Pharmacia Biotech, Milan, Italy) for at least 1 h in 40% 2-propanol and de-stained with a solution containing 5% acetic acid until clear bands of gelatinolysis appeared on a dark background. Matrix metalloproteases 2 and 4 (MMP2 and MMP9) were measured using Image Lab software and the % of pixels were normalized versus the number of cells in each sample.

2.8. Soft agar assay

Soft agar assay was used in order to analyse the effect of tolvaptan on anchorage independent growth of H69 cells by preparing a multilayer plate. The bottom layer was obtained by mixing 500 μl of pre-warmed culture medium and 500 μl of 1% noble autoclaved agar. Once the lower layer of agar had solidified, the upper layer was prepared by mixing 500 μl of RPMI 1640 double added with FBS and 500 μl of 0.6% noble autoclaved agar. In addition, in the upper layer three different concentrations of tolvaptan (20 μM, 40 μM, 50 μM) were mixed together with 50,000 cells per well. The experiments were performed in 6-well plates and the time required for adequate colony formation was set around 21 days. Finally, the number of colonies in each well was counted by using a light microscope after staining with 0.1% crystal violet solution. Colonies were counted by manually drawing squares underneath the plate for visible demarcation and the colony count was plotted from the average of 16 different fields per well.

2.9. RNA isolation and quantitative RT-PCR analysis

Total RNA was extracted by using Tri Reagent with DNAse treatment, according to the manufacturer's instruction, and samples were quantified by measuring the absorbance at 260 nm (Nanodrop, Wilmington, DE, USA). cDNA prepared from total RNA (Taqman Reverse Transcription Reagents, Applied Biosystem Inc., Foster City, CA, USA) was used to assess the expression of target genes and quantitatively analysed by real-time RT-PCR by using pre-developed TaqMan Assays. The probes were Assay-On-Demand products (Applied Biosystem Inc., Foster City, CA, USA) for HMOX1 (Hs01110250); ROCK-1 (Hs 00178463_m1), ROCK-2 (Hs00153074_m1) and RHOA, (Hs00357608_m1). The mRNA quantitation was based on the comparative Ct (for cycle threshold) method and normalized to 18S RNA (Hs03003631_g1). Results were expressed as target mRNA fold increase compared with control. All measurements were carried out in triplicates and at least two independent experiments were performed.

2.10. Western Blot analysis

Cells were lysed in RIPA lysis buffer supplemented with complete protease and phosphatase inhibitor cocktail and the protein concentrations were determined using a Bradford protein assay. Cell lysates (40 μg of proteins) were fractionated by Mini-PROTEAN TGX Stain-Free Precast Gels (Biorad, Hercules. CA, USA), an imaging technology that utilizes a polyacrylamide gel containing a proprietary trihalo compound to make proteins fluorescent directly in the gel. The PVDF membranes were blocked with 5% milk and incubated with specific primary antibodies as follows: rabbit monoclonal anti-Cofilin (5175 Cell signalling, Danvers, MA, USA), rabbit monoclonal anti-phospho-Cofilin (Ser3) (3313 Cell signalling, Danvers, MA, USA), rabbit monoclonal anti HMOX-1 (ab52947, Abcam, Cambridge, UK), rabbit monoclonal anti RhoA (#2117, Cell signalling Danvers, MA, USA), rabbit polyclonal anti AVPR2 (#75409, Invitrogen, Carlsbad, CA, USA), mouse monoclonal anti Cyclin D1 (#8396, Santa Cruz Biotechnology Inc, Dallas, TX, USA), rabbit monoclonal anti AKT (#SAB4500800, Sigma-Aldrich, Saint Louis, MO, USA), mouse monoclonal anti phospho-AKT (05-1003, Millipore, Burlington, MA, USA), rabbit polyclonal anti PKA (PA5-17626, Thermofisher Scientific, Walthan, MA, USA). This step was followed by a subsequent incubation with a secondary antibody conjugated to horseradish peroxidase. Chemiluminescent Images were acquired with a Bio-Rad ChemiDoc Imaging System (Biorad, Hercules, CA, USA) and through ImageJ Software. Proteins of interest were quantified and normalized versus stain free acquisition.

2.11. Reactive oxygen species analysis

Flow cytometry determination of reactive oxygen species (ROS) was performed using a Muse cytometer (Guava® Muse® Cell Analyser, Luminex Technology, Austin, TX, USA) after loading the cells with 5 μM Cell ROX Reagent (Green Dye). The cells were incubated for 30 min at 37 °C and then wells were washed twice with HBSS to remove any remaining unincorporated dye. Finally, cells were rapidly trypsinized and 1×10^6 cells were resuspended in 100 μl of HBSS supplemented with FBS 10% and immediately analysed. Menadione is a cytotoxic quinone that generates superoxide and it was added to cell medium to a final concentration of 100 μM for 2 h at 37 °C in a humidified atmosphere (5% CO2/95% air), as positive control. The cell fluorescence intensity was measured using 485/520 nm absorption/emission filters. A total of 10,000 events were acquired for each analysis and results show two different populations: live cells (M1- ROS negative) and cell exhibiting ROS (M2- ROS positive).

2.12. Statistical analysis

Data are expressed as mean ± SEM unless otherwise indicated. Student's t-test was used for comparing two classes of data, while oneway Anova were calculated to compare multiple experiments. Differences were considered as statistically significant if p values ≤ 0.05.

3. Results

3.1. Cell proliferation and apoptosis in low [Na^+]

Cell proliferation was assessed by WST-8 assay. We found that in low [Na^+] H69 cells proliferation was significantly increased compared to normal [Na^+] for these cells (i.e. 153 mM) (Fig. 1A).

The PI3-K/AKT pathway was examined by Western Blot analysis. PI3-K is constitutively active in H69 cells (Moore et al., 1998). Total AKT was found to be increased in low [Na^+], whereas no difference was found in p-AKT (Ser^{473}) expression (Fig. 1B).

The analysis of cell cycle showed a significant reduction of G0/G1

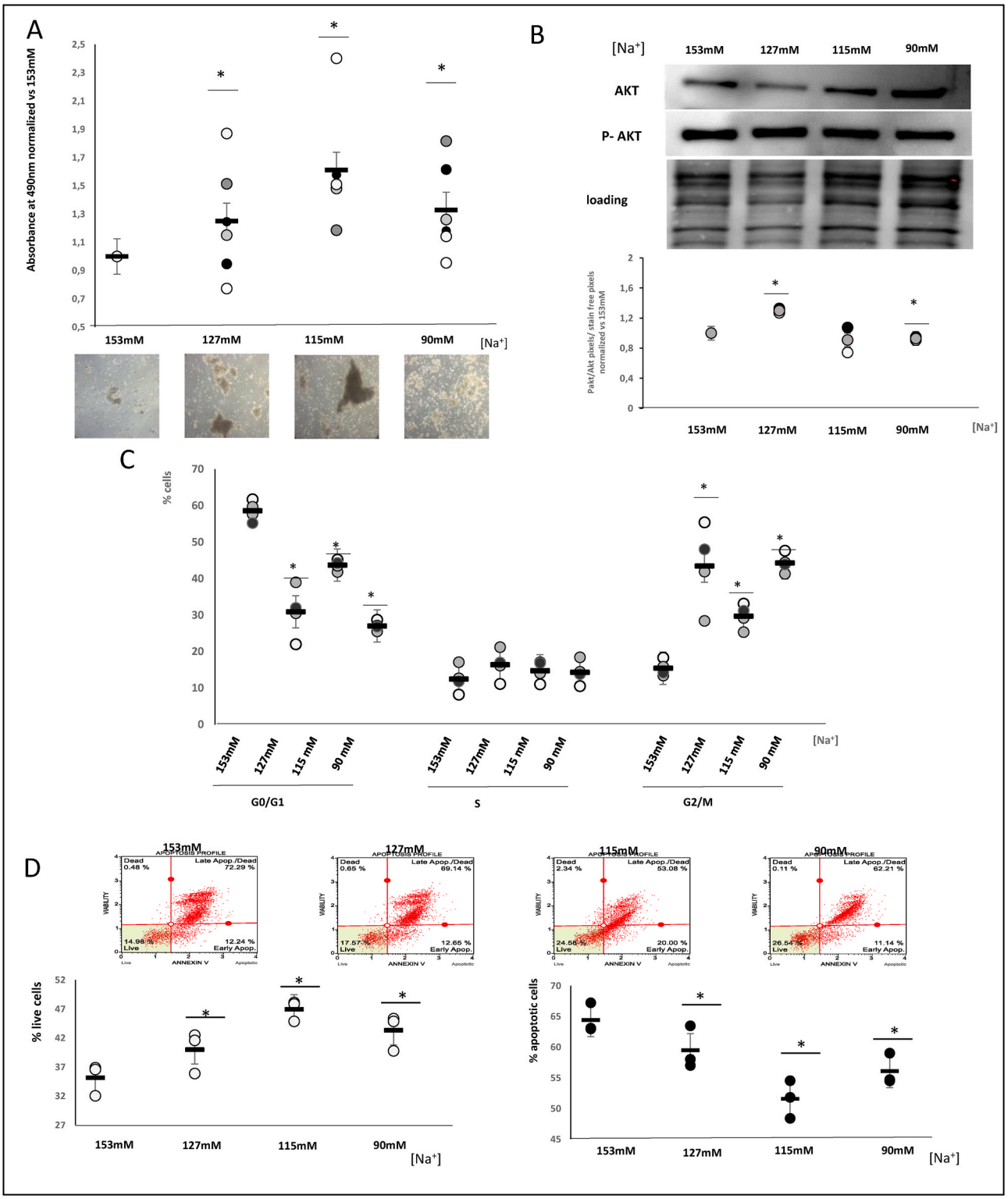

Fig. 1. Effect of low extracellular [Na+] on H69 cells proliferation, cell cycle and apoptosis. **A)** H69 cell proliferation was assessed by using WST1. Results are expressed as mean ± SE of the optical density (OD) at 490 nm/well at different [Na^+], normalized versus control ([Na^+] 153 mM). **B)** Western Blot analysis of AKT/P-AKT. The plot represents the P-AKT/AKT ratio, normalized versus [Na^+] 153 mM. Results are expressed as mean ± SE. **C-D)** The effects of sodium decrease on cell cycle and apoptosis were assessed by cytofluorimetry and results are expressed as mean ± SE of the percentage of cells in G0/G1, S and G2/M phase (C) and % of live and dead cells (D). (* = $p \leq 0.05$ *vs* [Na^+] 153 mM).

H69 cells in low [Na^+] and a significant increase of G2/M cells, compared to cells cultured in normal [Na^+] (Fig. 1C).

The evaluation of apoptotis by annexinV/PI analysis revealed that the percentage of apoptotic cells (early + late) significantly decreased in low [Na^+], compared to normal [Na^+], whereas the number of live cells increased (Fig. 1D).

3.2. Cell invasion in low [Na^+]

H69 cells showed an increased ability to cross matrigel-coated

membranes in cell invasion assays, when cultured in reduced [Na^+]. In particular, a significant increase was present at a [Na^+] of 127 mM and was confirmed at 115 mM and 90 mM (Fig. 2A).

The effect of low [Na^+] on H69 cells invasiveness was confirmed by a zymography assay, in which the activity of collagenases type 4 (i.e. MMP-2 and MMP-9) was analysed. As shown in Fig. 2B, there was a significant increase of the enzymatic activity of MMP-9 at a [Na^+] of 127 mM and 115 mM, and a significant increase of the enzymatic

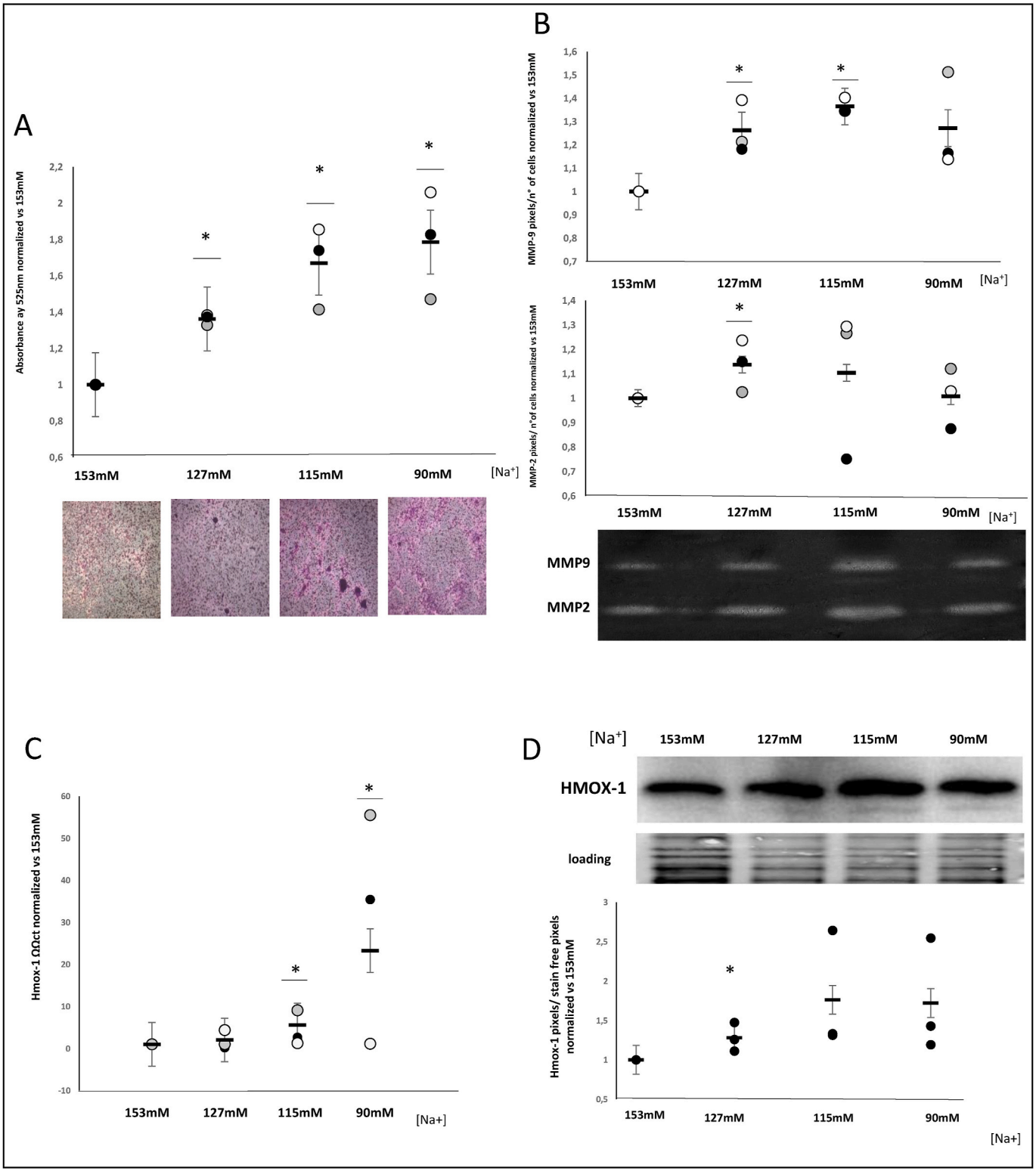

Fig. 2. Effect of low extracellular [Na^+] on cell invasion and HMOX-1 expression. **A)** Cell invasion assay. Migrated cells were evaluated using matrigel coated invasion membranes. The images are representative of invading cells. **B)** Collagenase type IV production was analysed using zymography assay. Images show the areas of gels degradated by MMPs and plots represent the mathematical ratio of pixels/cells number. **C)** HMOX-1 mRNA expression was quantified by Real time qRT-PCR. **D)** HMOX-1 proteins levels, as assessed by Western blot analysis. Results are expressed as mean ± SE. (* = $p \leq 0.05$ *vs* [Na^+] 153 mM).

activity of MMP-2 at a [Na^+] of 127 mM.

3.3. Heme oxygenase-1 expression in low [Na^+]

The induction of heme oxygenase-1 (HMOX-1) expression has been associated to cell exposure to low extra-cellular [Na^+] *in vitro* (Barsony et al., 2011; Benvenuti et al., 2013; Marroncini et al., 2020). Similar to previous evidence, the amount of HMOX-1 RNA, as assessed by RT-PCR, showed a stepwise increase in H69 cells exposed to reduced [Na^+] (Fig. 2C). Accordingly, HMOX-1 protein expression appeared increased in low [Na^+] (Fig. 2D).

3.4. RhoA/ROCK1/ROCK2 pathway in low [Na^+]

RhoA, ROCK1 and ROCK2 are involved in the regulation of actin cytoskeleton and in the promotion of cofilin-mediatyed actin polymerization. Stress-induced actin cytoskeleton remodeling events lead to cell detachment and cancer progression (Shi et al., 2013).

As shown in Fig. 3A, in H69 cells the amount of mRNA for RhoA, ROCK1 and ROCK2 was increased in low [Na^+] compared to normal [Na^+]. RhoA and ROCK-1 protein levels were also assessed and appeared increased in reduced [Na^+] (Fig. 3B). The downstream effect of the activation of the RhoA/ROCK1/2 pathway was confirmed by the increased cofilin/P-cofilin ratio when cells were exposed to reduced [Na^+] compared to normal [Na^+] (Fig. 3C).

3.5. Tolvaptan, cell proliferation and apoptosis

The effect of the V_2 receptor antagonist tolvaptan on H69 cell proliferation was tested. These cells are known to express the V_2 receptor, as it was preliminarily confirmed by Western blot analysis (Fig. 4A). We found that tolvaptan dose- and time-dependently reduced the rate of cell proliferation, with an IC_{50} of. 53.6 μM at 48 h (Fig. 4B) in cells grown in normal [Na^+]. In all the following experiments cells were exposed to tolvaptan for 48 h.

With regard to cell cycle, tolvaptan (20 μM, 40 μM, 50 μM) determined an increase of the percentage of G0/G1 cells and a decrease of S and G2/M cells (Fig. 4C). Accordingly, the expression of cyclin D1 was found to be significantly decreased after treatment with increasing doses of tolvaptan. Protein expression of PKA, i.e. the first key regulator of the V_2 receptor signalling pathway, was also evaluated and was found to be decreased by tolvaptan exposure in H69 cells. The PI3K/AKT pathway was also analysed. Total AKT significantly decreased upon treatment with increasing doses of tolvaptan, whereas its phosphorylated amount (Ser^{473}) remained unchanged (Fig. 4D).

Growth in soft agar was also assessed, in order to evaluate the effect of tolvaptan on cell anchorage-independent growth. Tolvaptan exposure was associated with a significant reduction of the ability of H69 cells to proliferate and form colonies in this condition (Fig. 5A). Furthermore, tolvaptan (20 μM, 40 μM, 50 μM) caused a significant increase in the number of apoptotic cells and a reduction of live cells (Fig. 5B).

The generation of ROS is known to play an important role in modulating apoptosis (Aggarwal et al., 2019; Gao et al., 2020). Hence, the amount of intracellular ROS was evaluated and was found to be increased in cells exposed to tolvaptan (Fig. 5C).

3.6. Tolvaptan and cell invasion

Tolvaptan effectively counteracted the ability of H69 cells to cross matrigel-coated membranes (Fig. 6A). The effect of tolvaptan on cell invasiveness was confirmed by zymography. In particular, the expression of MMP-2 and MMP-9 was reduced by tolvaptan (Fig. 6B).

3.7. Tolvaptan and RhoA/ROCK1/ROCK2 pathway

In view of the role of the RhoA/ROCK1/ROCK2 pathway in the regulation of cell movement through the remodeling of actin cytoskeleton and of the aforementioned results on the activation of this pathway in H69 cells cultured in low [Na^+], we evaluated ROCK1, ROCK2 and RhoA expression in cells exposed to tolvaptan. Cells treated with tolvaptan showed a reduced mRNA expression of RhoA, ROCK1and ROCK2 compared to untreated cells (Fig. 7A). Accordingly, the protein expression of RhoA and ROCK1 proteins was significantly decreased by tolvaptan treatment (Fig. 7B). Furthermore, the cofilin/P cofilin ratio was found to be decreased (Fig. 7C).

4. Discussion

Hyponatraemia has been related to a worse outcome in patients affected by cancer, and we have recently demonstrated that cells from different tumors show an increased proliferation rate and invasiveness when cultured in reduced extra-cellular [Na^+] (Marroncini et al., 2020).

In this study we first evaluated the effect of low extra-cellular [Na^+] in SCLC cells (i.e. H69). SCLC is the tumor that is most commonly associated with hyponatraemia, mainly due to the ectopic secretion of AVP (Castillo et al., 2016). The choice of this cell line was motivated by the fact that they are the SCLC cells that have been most frequently used for *in vitro* studies, they have been isolated by the primary tumor and not by metastases and express the V_2 receptor, which was necessary for the second part of our study.

We found that the proliferation rate of H69 cells significantly increased in low [Na^+] compared to normal [Na^+]. We also investigated the PI3K/AKT pathway. PI3K is constitutively active in H69 cells (Moore et al., 1998). AKT modulates a variety of biological functions, including cell survival and growth by regulating both post-translational mechanisms and gene transcription (Zinda et al., 2001; Pérez-Ramírez et al., 2015). Upon exposure to low [Na^+], total AKT was increased and, on the other hand, the amount of phosphorylated (Ser^{473}) and active form (Moore et al., 1998) was found unchanged.

In agreement with these findings, cell cycle analysis showed that cells exposed to reduced [Na^+] were predominantly distributed in the G2/M phase, which is the turning point of cell mitosis. On the other hand, the number of apoptotic cells significantly decreased in low [Na^+], whereas live cells increased.

Besides the increased proliferation rate, cells maintained in reduced [Na^+] showed a greater invasive potential, as assessed by the ability to cross matrigel-coated filters, which was paralleled by an increased activity of MMP-2 and MMP-9.

It has been demonstrated that reduced [Na^+] is associated with an increased expression of HMOX-1 (Barsony et al., 2011; Benvenuti et al., 2013), which has been related to different critical steps involved in lung cancer biology, such as the creation of a permissive microenvironment for carcinogenesis, cell proliferation and survival, invasion, angiogenesis, immune suppression, chemoresistance (Hemmati et al., 2021). Interestingly, selective inhibition of HMOX-1 has been proven to effectively reduce cell proliferation, angiogenesis and invasion, and to induce apoptosis in cancer cells *in vitro* and *in vivo* (Abdalla et al., 2019; Hemmati et al., 2021). Thus, HMOX-1 has been considered as a potential target for designing new anticancer strategies. In agreement with our previous observations in different cancer cell lines (i.e. neuroblastoma, pancreas carcinoma, ileo-cecal adenocarcinoma, chronic myeloid leukemia), in the present study we found that low [Na^+] induced the expression of HMOX-1 in H69 cells, too.

Furthermore, it is well known that the RhoA/ROCK pathway plays an important role in modulating cell proliferation and motility. RhoA is a small GTPase, which is coupled to membrane receptors. It acts as a molecular switch for the reorganization of actin and the remodeling of the cytoskeleton. ROCK1 and ROCK2 are Rho-associated proteins with kinase activity and their activation leads to the phosphorylation of actin cytoskeleton-associated proteins, such as cofilin (Tanaka et al., 2018). Cofilin activation/inactivation is modulated by changes in the balance of kinases, phosphatases and other cofilin-related regulatory proteins.

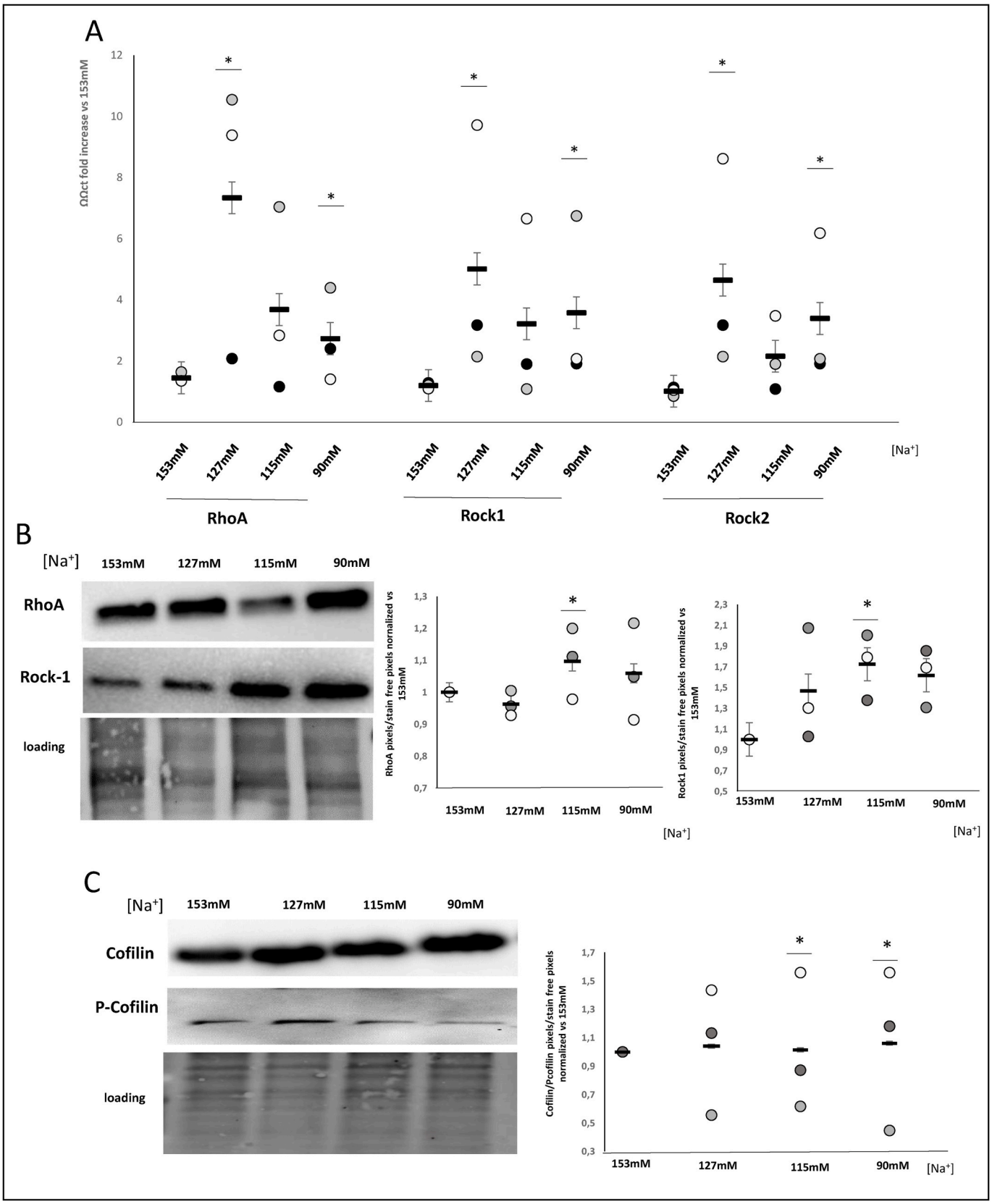

Fig. 3. Effect of low extracellular [Na^+] on RhoA/Rock1-2 pathway. **A)** RHOA, ROCK1 and ROCK2 mRNA levels in H69 cells, determined by Real time qRT-PCR. The results are expressed as Δct fold increased at different [Na^+] versus 153 mM. **B)** RhoA and ROCK1 protein expression levels. **C)** Cofilin and P-cofilin protein expression levels. The plot represents the cofilin/P-cofilin ratio, normalized versus 153 mM. Results are expressed as mean ± SE (* = $p \leq 0.05$ *vs* [Na^+] 153 mM).

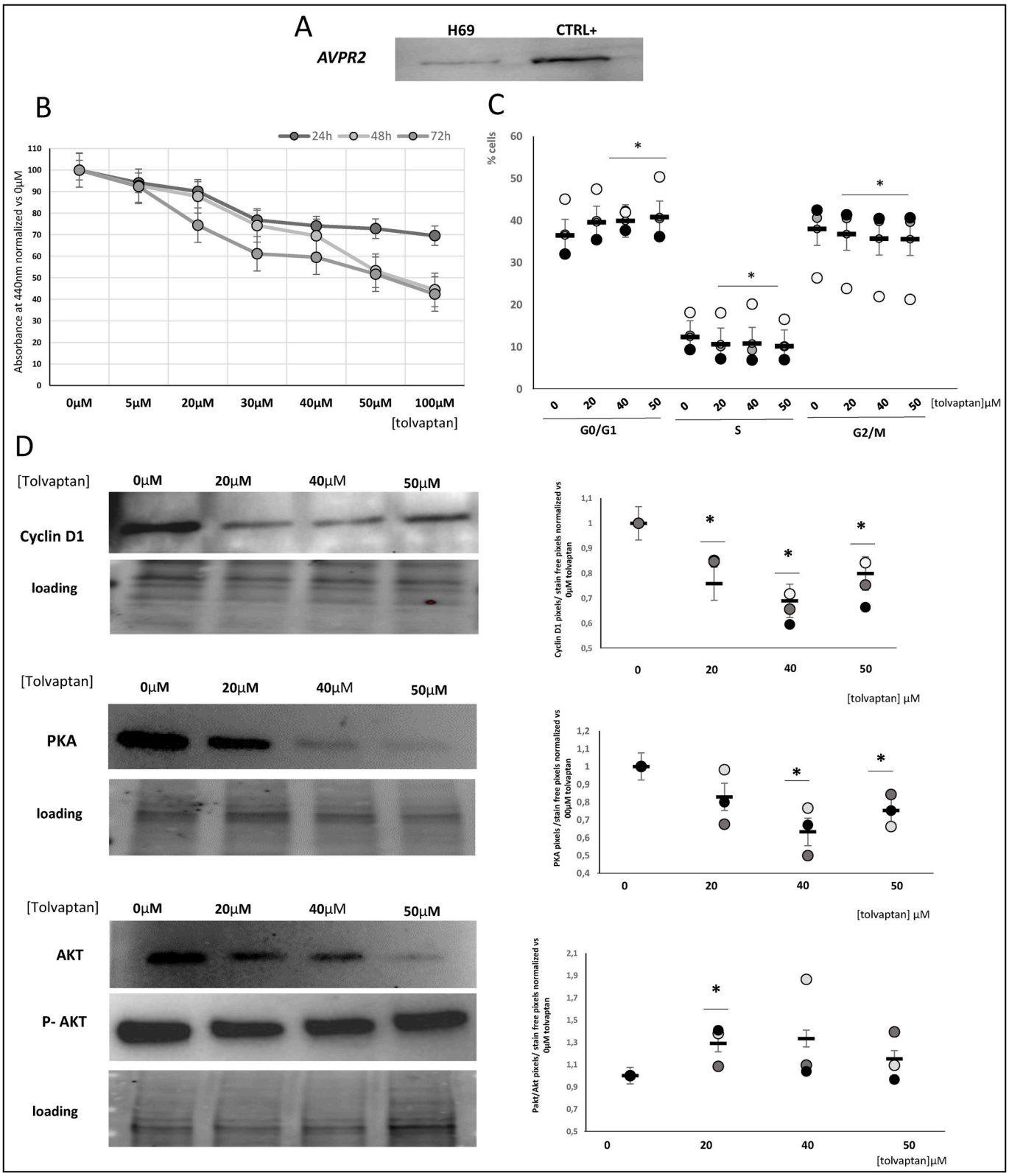

Fig. 4. Effect of tolvaptan on H69 cell proliferation. **A)** V_2 receptor expression in H69 cells. CTRL+ = human kidney cells, used as positive control. **B)** Dose response curve of tolvaptan on H69 cell proliferation, as assessed by WST-8 assay. **C)** Effects of different concentrations of tolvaptan on cell cycle. **D)** Western Blot analysis of cyclin D1, PKA, protein kinase B (AKT) and phospho-protein kinase B (p-AKT) in H69 cells exposed to tolvaptan. (* = $p \leq 0.05$ vs cells not exposed to tolvaptan, 0 µM).

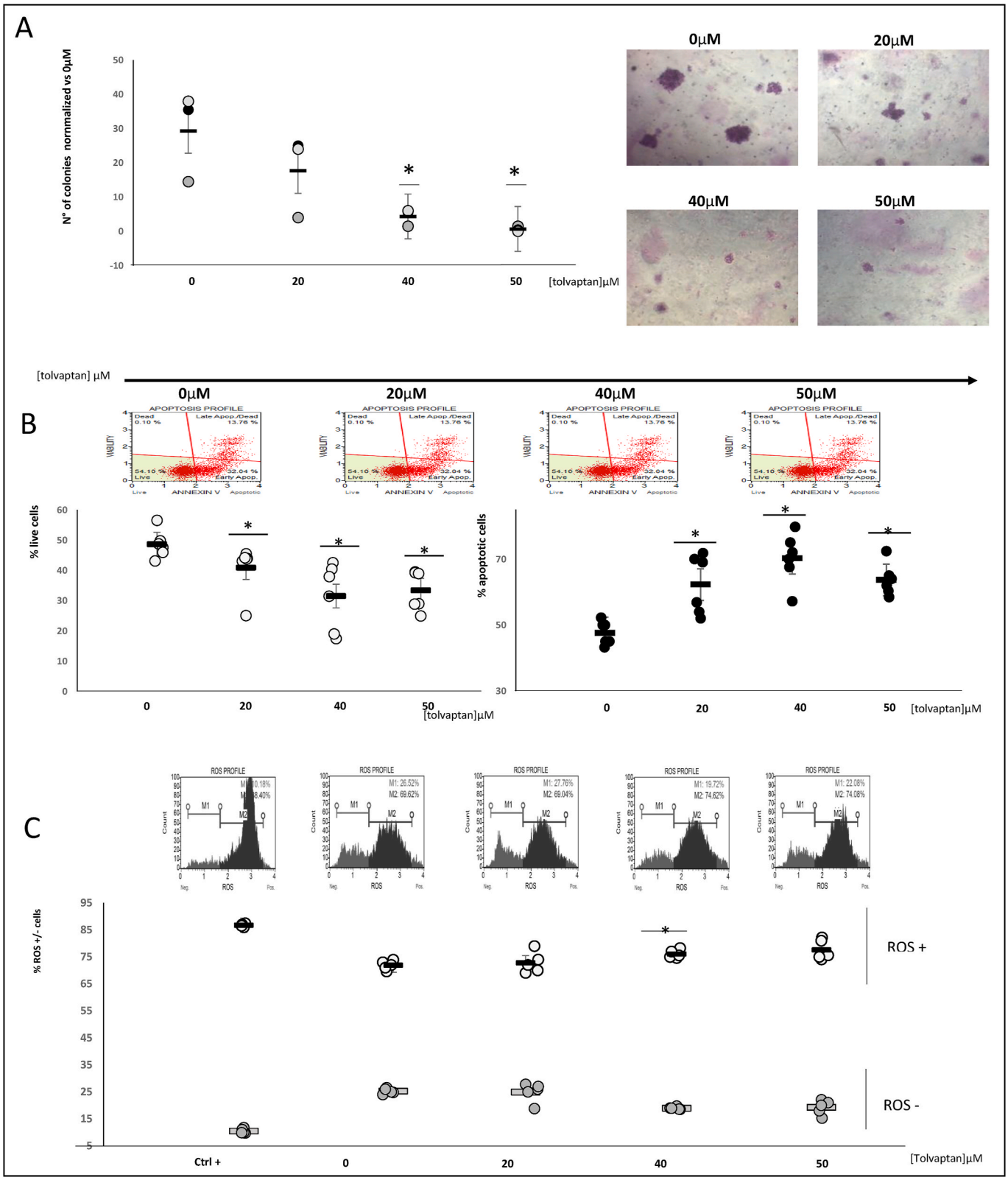

Fig. 5. Effect of tolvaptan on colony formation, apoptosis and ROS production. **A)** Effect of tolvaptan on anchorage independent growth. The scatter plot shows the number of H69 colonies (mean ± SE) counted in each wells, normalized versus control and the images are representative of the colonies. **B)** Effect of tolvaptan on H69 cells apoptosis through the analysis of annexin V expression. The scatter plots indicate live and total apoptotic cells in control and treated cells. **C)** Effect of tolvaptan on ROS accumulation. Representative top quadrant analysis of CellROX Green Reagent-loaded cells treated with menadione as positive control and with different concentrations of tolvaptan. The scatter plots indicate the percentage of ROS+ and ROS – H69 cells. (* = $p \leq 0.05$ vs cells not exposed to tolvaptan, 0 μM).

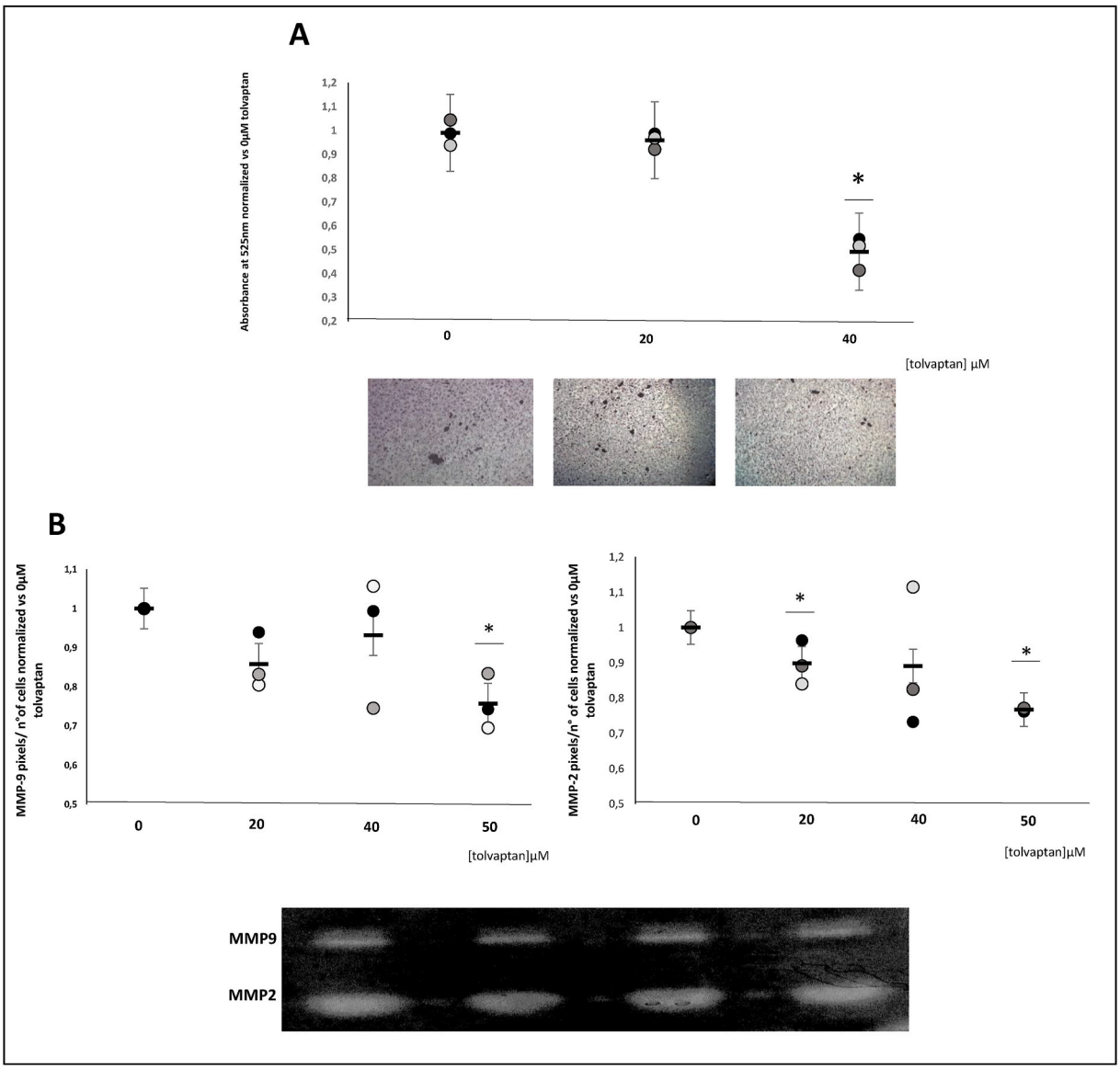

Fig. 6. Effect of tolvaptan on H69 cells invasion. **A)** Cell invasion assay. Migrated cells were evaluated using matrigel coated invasion membranes. The images are representative of invading cells. **B)** Collagenase type IV production was analysed using zymography assay. Images show the areas of gels degraded by MMPs and scatter plots represent the mathematical ratio of pixels/cells number of MMP2 and MMP9 respectively. (* = $p \leq 0.05$ vs cells not exposed to tolvaptan, 0 μM).

These changes are responsible for the initiation of the early steps that lead to cancer invasion and metastasization. H69 cells showed an increased expression of RhoA/ROCK1/2 kinases and a decreased phosphorylation of cofilin at Ser3, when cultured in low [Na^+], in agreement with our previous findings (Marroncini et al., 2020). It has been demonstrated that differential activation of the cofilin regulators ROCK1, LIMK1 and SSH1L, and cofilin dephosphorylation, can promote microtentacles formation and enhance metastatic risk (Aggelou et al., 2018). Hence, the increased total cofilin/P cofilin ratio observed in H69 cells cultured in low [Na^+] is expected to promote the formation of actin filaments from actin monomers. A deregulation of the RhoA/ROCK1/2 pathway has been observed in different human cancers, such as T-cell lymphoma, neuroblastoma and gastric carcinoma (Dyberg et al., 2017; Kakiuchi et al., 2014; Sakata-Yanagimoto et al., 2014).

Overall, the afore mentioned findings clearly indicate that reduced [Na^+] promotes cell proliferation and survival of H69 cells, together with increased invasiveness. These features are associated with the induction of the expression of HMOX-1 and the activation of the RhoA/ROCK1/2 pathway.

As already mentioned, SCLC is frequently associated with hyponatraemia secondary to SIAD (Castillo et al., 2016). Besides the presence of ectopic secretion of AVP by tumoral cells, in SCLC patients SIAD may be also elicited by platinum-based therapies (Wu et al., 2020). Noteworthy, hyponatraemia is associated with a more severe outcome in patients affected by SCLC, as well as by other malignancies (Berardi et al., 2019; Hansen et al. 2010; Tiseo et al., 2014; Kobayashi et al., 2014). V_2 receptor antagonists have been approved for the treatment of SIAD more than a decade ago and have been found to effectively correct hyponatraemia in different clinical settings (Berl et al., 2010; Bhandari et al., 2017; Greenberg et al., 2015; Peri, 2013; Schrier et al., 2006). Other treatment strategies for hyponatraemia secondary to SIAD, such as fluid restriction, may be problematic in cancer patients. In particular, chemotherapy requires the infusion of large volumes of fluids and therefore serum [Na^+] cannot be controlled by limiting fluid intake. Hence, vaptans appeared to have a proper space in the treatment of hyponatraemia in these patients. Interestingly, treatment with vaptans has been associated with reduced length of stay in the hospital, reduced risk of rehospitalization and improved quality of life (Petereit et al.,

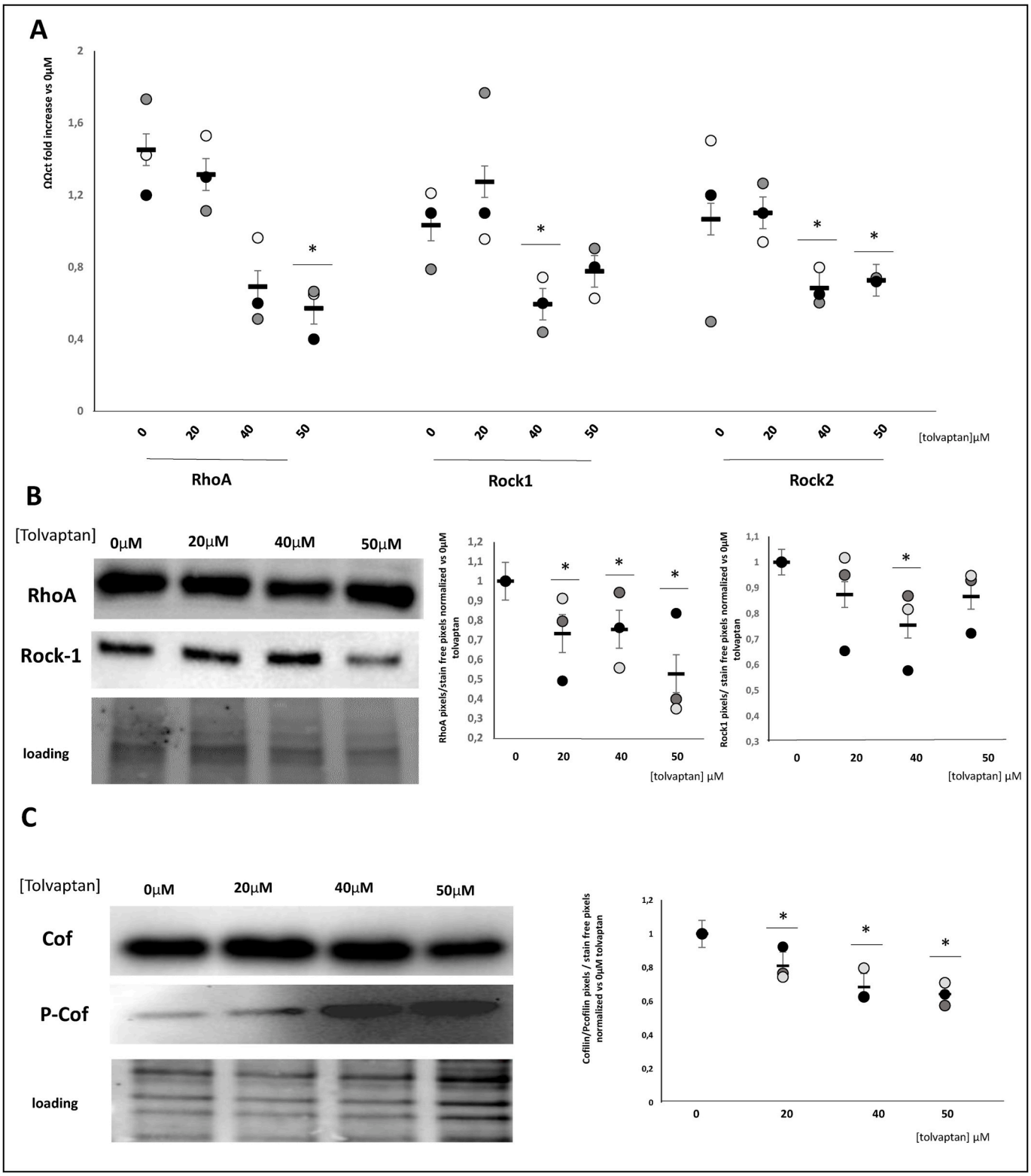

Fig. 7. Effect of tolvaptan on RhoA/ROCK1-2 signalling. **A)** mRNA expression levels of RhoA, ROCK1 and ROCK2 **B)** RhoA and ROCK1 protein expression levels. **C)** Cofilin (Cof) and P-cofilin (P-Cof) protein expression levels. The plots represent the cofilin/P-cofilin ratio. Results are expressed as mean ± SE. (* = $p \leq 0.05$ vs cells not exposed to tolvaptan 0 μM).

2013; Berardi et al., 2019).

Based on the known effects of tolvaptan in counteracting renal cysts growth in PKD (Torres et al, 2012, 2017) and on the anti-proliferative effects observed in hepatocellular and renal carcinoma cells (Sinha et al., 2020; Wu et al., 2015), in our study we evaluated the effects of tolvaptan in SCLC cells. H69 cells express the V_2 receptor and therefore are a target for evaluating the effects of vaptans. Noteworthy, we found that tolvaptan effectively reduced cell proliferation with an IC_{50} of about 50 μM. In addition, we demonstrated that tolvaptan caused an increase of the number of cells in G0/G1 phase, whereas cells in S or G2/M phase

appeared decreased. Accordingly, the expression of cyclin D1 was significantly reduced.

Furthermore, tolvaptan exposure effectively decreased the amount of PKA protein, which is the first critical step of the V_2 receptor signalling. With regard to AKT/pAKT expression, following tolvaptan exposure total AKT was significantly reduced, whereas p-AKT remained unchanged. This finding, together with the results of AKT/pAKT expression in low [Na^+], indicates that low [Na^+] and tolvaptan have opposite effects on the amount of AKT, yet p-AKT expression does not change because of the constitutive activation of PI3-K in H69 cells (Moore et al., 1998).

H69 cells were able to form colonies in soft agar, which is a peculiar feature of cancer cells. However, tolvaptan exposure markedly reduced the anchorage-independent growth of these cells. Moreover, the percentage of apoptotic cells significantly increased when tolvaptan was added to the culture medium. Interestingly enough, apoptosis was associated with an increased production of intracellular ROS, which are known to play an important role in modulating apoptosis (Aggarwal et al., 2019; Gao et al., 2020). In particular, ROS participate in the interplay between autophagy and apoptosis by modulating the redox signalling pathways and elevated levels of ROS ultimately lead to apoptosis. It is also known that apoptosis in cancer cells can be triggered by anticancer molecules via the generation of ROS (Gao et al., 2020).

Finally, we demonstrated that tolvaptan counteracted cell invasion, as indicated by a significant reduction of the ability of H69 cells to cross matrigel-coated membranes. Accordingly, the RhoA/ROCK-1/ROCK2 pathway, which is involved in regulating cell invasiveness, was inhibited by tolvaptan exposure. Consequently, the cofilin/P cofilin ratio appeared decreased.

In our study we used tolvaptan concentrations ranging from 20 to 50 μM and in most cases we observed significant effects at the lowest concentration. Noteworthy, in the experiments for the determination of the IC_{50} of tolvaptan, we observed a reduced rate of cell proliferation already at 5 μM. Similar concentrations of tolvaptan have been reported to determine antitumoral effects in hepatocarcinoma (Wu et al., 2015) and in renal cancer cells (Sinha et al., 2020). It has been shown that the serum peak concentration after a single 30 mg dose of tolvaptan in healthy subjects is in the low micromolar range (0.5–0.7 μM) (Shoaf et al., 2012).

Overall, our results indicate for the first time that low [Na^+] favours proliferation and invasivity of a SCLC cell line. Although limited to a single cell line, these findings are in agreement with similar results obtained in other cancer cell lines (Marroncini et al., 2020) and with the clinical observation that hyponatraemia is a predictor of a worse outcome in patients affected by SCLC. Furthermore, we demonstrated that the V_2 receptor antagonist tolvaptan, which was originally approved for the treatment of hyponatraemia secondary to SIAD, effectively reduces proliferation, survival and invasivity of SCLC (H69) cells. It remains to be investigated the effect of tolvaptan in cells grown in reduced [Na^+]. In addition, these data need to be confirmed in other cancer cell lines *in vitro* and also using *in vivo* xenografts. However, our original findings, together with the published data on the effect of tolvaptan in hepatocellular and renal carcinoma cells (Sinha et al., 2020; Wu et al., 2015), suggest a potential role of tolvaptan in anti-cancer strategies, likely due to a dual effect: correction of hyponatremia, when present, and reduction of cell proliferation and invasivity. We may then speculate that tolvaptan promises to be more effective in limiting tumoral spread than other strategies that are available to correct hyponatremia.

Funding

This research was supported by grants from Otsuka Pharmaceutical Europe Ltd. and PRIN 2017R5ZE2C.

CRediT authorship contribution statement

Giada Marroncini: Conceptualization, Investigation, Formal analysis, Writing – original draft. **Cecilia Anceschi:** Conceptualization, Investigation, Formal analysis, Writing – original draft. **Laura Naldi:** Investigation. **Benedetta Fibbi:** Conceptualization, Writing – review & editing. **Federica Baldanzi:** Investigation. **Serena Martinelli:** Investigation. **Simone Polvani:** Investigation. **Mario Maggi:** Writing – review & editing. **Alessandro Peri:** Conceptualization, Supervision, Funding acquisition, Writing – original draft, Writing – review & editing, Supervision, Project administration.

Declaration of competing interest

The authors do not have anything to disclose.

References

Abdalla, M.Y., Ahmad, I.M., Rachagani, S., Banerjee, K., Thompson, C.M., Maurer, H.C., Olive, K.P., Bailey, K.L., Britigan, B.E., Kumar, S., 2019. Enhancing responsiveness of pancreatic cancer cells to gemcitabine treatment under hypoxia by heme oxygenase-1 inhibition. Transl. Res. 207, 56–69. https://doi.org/10.1016/j.trsl.2018.12.008.

Aggarwal, V., Tuli, H.S., Varol, A., Thakral, F., Yerer, M.B., Sak, K., Varol, M., Jain, A., Khan, M.A., Sethi, G., 2019. Role of reactive oxygen species in cancer progression: molecular mechanisms and recent advancements. Biomolecules 9. https://doi.org/10.3390/biom9110735.

Aggelou, H., Chadla, P., Nikou, S., Karteri, S., Maroulis, I., Kalofonos, H.P., Papadaki, H., Bravou, V., 2018. LIMK/cofilin pathway and Slingshot are implicated in human colorectal cancer progression and chemoresistance. Virchows Arch. 472, 727–737. https://doi.org/10.1007/s00428-018-2298-0.

Balachandran, K., Okines, A., Gunapala, R., Morganstein, D., Popat, S., 2015. Resolution of severe hyponatraemia is associated with improved survival in patients with cancer. BMC Canc. 15, 163. https://doi.org/10.1186/s12885-015-1156-6.

Barsony, J., Sugimura, Y., Verbalis, J.G., 2011. Osteoclast response to low extracellular sodium and the mechanism of hyponatremia-induced bone loss. J. Biol. Chem. 286, 10864–10875. https://doi.org/10.1074/jbc.M110.155002.

Benvenuti, S., Deledda, C., Luciani, P., Modi, G., Bossio, A., Giuliani, C., Fibbi, B., Peri, A., 2013. Low extracellular sodium causes neuronal distress independently of reduced osmolality in an experimental model of chronic hyponatremia. NeuroMolecular Med. 15, 493–503. https://doi.org/10.1007/s12017-013-8235-0.

Berardi, R., Caramanti, M., Castagnani, M., Guglielmi, S., Marcucci, F., Savini, A., Morgese, F., Rinaldi, S., Ferrini, C., Tiberi, M., Torniai, M., Rovinelli, F., Fiordoliva, I., Onofri, A., Cascinu, S., 2015a. Hyponatremia is a predictor of hospital length and cost of stay and outcome in cancer patients. Support. care cancer off. J. Multinatl. Assoc. Support. Care Canc 23, 3095–3101. https://doi.org/10.1007/s00520-015-2683-z.

Berardi, R., Caramanti, M., Fiordoliva, I., Morgese, F., Savini, A., Rinaldi, S., Torniai, M., Tiberi, M., Ferrini, C., Castagnani, M., Rovinelli, F., Onofri, A., Cascinu, S., 2015b. Hyponatraemia is a predictor of clinical outcome for malignant pleural mesothelioma. Support. care cancer off. J. Multinatl. Assoc. Support. Care Canc 23, 621–626. https://doi.org/10.1007/s00520-014-2398-6.

Berardi, R., Mastroianni, C., Lo Russo, G., Buosi, R., Santini, D., Montanino, A., Carnaghi, C., Tiseo, M., Chiari, R., Camerini, A., Barni, S., De Marino, V., Ferrari, D., Cristofano, A., Doni, L., Freddari, F., Fumagalli, D., Portalone, L., Sarmiento, R., Schinzari, G., Sperandi, F., Tucci, M., Inno, A., Ciuffreda, L., Mariotti, M., Mariani, C., Caramanti, M., Torniai, M., Gallucci, R., Bennati, C., Bordi, P., Buffoni, L., Galeassi, A., Ghidini, M., Grossi, E., Morabito, A., Vincenzi, B., Arvat, E., 2019. Syndrome of inappropriate anti-diuretic hormone secretion in cancer patients: results of the first multicenter Italian study. Ther. Adv. Med. Oncol. 11 https://doi.org/10.1177/1758835919877725, 1758835919877725.

Berardi, R., Rinaldi, S., Caramanti, M., Grohè, C., Santoni, M., Morgese, F., Torniai, M., Savini, A., Fiordoliva, I., Cascinu, S., 2016a. Hyponatremia in cancer patients: time for a new approach. Crit. Rev. Oncol. Hematol. 102, 15–25. https://doi.org/10.1016/j.critrevonc.2016.03.010.

Berardi, R., Santoni, M., Rinaldi, S., Nunzi, E., Smerilli, A., Caramanti, M., Morgese, F., Torniai, M., Savini, A., Fiordoliva, I., Onofri, A., Pistelli, M., Taccaliti, A., Cascinu, S., 2016b. Risk of hyponatraemia in cancer patients treated with targeted therapies: a systematic review and meta-analysis of clinical trials. PloS One 11, e0152079. https://doi.org/10.1371/journal.pone.0152079.

Berl, T., Quittnat-Pelletier, F., Verbalis, J.G., Schrier, R.W., Bichet, D.G., Ouyang, J., Czerwiec, F.S., 2010. Oral tolvaptan is safe and effective in chronic hyponatremia. J. Am. Soc. Nephrol. 21, 705–712. https://doi.org/10.1681/ASN.2009080857.

Bhandari, S., Peri, A., Cranston, I., McCool, R., Shaw, A., Glanville, J., Petrakova, L., O'Reilly, K., 2017. A systematic review of known interventions for the treatment of chronic nonhypovolaemic hypotonic hyponatraemia and a meta-analysis of the vaptans. Clin. Endocrinol. 86, 761–771. https://doi.org/10.1111/cen.13315.

Castillo, J.J., Glezerman, I.G., Boklage, S.H., Chiodo 3rd, J., Tidwell, B.A., Lamerato, L. E., Schulman, K.L., 2016. The occurrence of hyponatremia and its importance as a prognostic factor in a cross-section of cancer patients. BMC Canc. 16, 564. https://doi.org/10.1186/s12885-016-2610-9.

Chawla, A., Sterns, R.H., Nigwekar, S.U., Cappuccio, J.D., 2011. Mortality and serum sodium: do patients die from or with hyponatremia? Clin. J. Am. Soc. Nephrol. 6, 960–965. https://doi.org/10.2215/CJN.10101110.

Corona, G., Giuliani, C., Parenti, G., Colombo, G.L., Sforza, A., Maggi, M., Forti, G., Peri, A., 2016. The economic burden of hyponatremia: systematic review and meta-analysis. Am. J. Med. 129, 823–835. https://doi.org/10.1016/j.amjmed.2016.03.007 e4.

Corona, G., Giuliani, C., Parenti, G., Norello, D., Verbalis, J.G., Forti, G., Maggi, M., Peri, A., 2013. Moderate hyponatremia is associated with increased risk of mortality: evidence from a meta-analysis. PloS One 8, e80451. https://doi.org/10.1371/journal.pone.0080451.

Corona, G., Giuliani, C., Verbalis, J.G., Forti, G., Maggi, M., Peri, A., 2015. Hyponatremia improvement is associated with a reduced risk of mortality: evidence from a meta-analysis. PloS One 10, e0124105. https://doi.org/10.1371/journal.pone.0124105.

Doshi, S.M., Shah, P., Lei, X., Lahoti, A., Salahudeen, A.K., 2012. Hyponatremia in hospitalized cancer patients and its impact on clinical outcomes. Am. J. kidney Dis. Off. J. Natl. Kidney Found. 59, 222–228. https://doi.org/10.1053/j.ajkd.2011.08.029.

Dyberg, C., Fransson, S., Andonova, T., Sveinbjörnsson, B., Lännerholm-Palm, J., Olsen, T.K., Forsberg, D., Herlenius, E., Martinsson, T., Brodin, B., Kogner, P., Johnsen, J.I., Wickström, M., 2017. Rho-associated kinase is a therapeutic target in neuroblastoma. Proc. Natl. Acad. Sci. U.S.A. 114, E6603–E6612. https://doi.org/10.1073/pnas.1706011114.

Farid, S.G., Prasad, K.R., 2015. Prognostic impact of hyponatraemia in patients with colorectal cancer. Color. Dis. Off. J. Assoc. Coloproctology Gt. Britain Irel. https://doi.org/10.1111/codi.12939.

Fucà, G., Mariani, L., Lo Vullo, S., Galli, G., Berardi, R., Di Nicola, M., Vernieri, C., Morelli, D., Dotti, K., Fiordoliva, I., Rinaldi, S., Gavazzi, C., Pietrantonio, F., Platania, M., de Braud, F., 2019. Weighing the prognostic role of hyponatremia in hospitalized patients with metastatic solid tumors: the HYPNOSIS study. Sci. Rep. 9, 12993 https://doi.org/10.1038/s41598-019-49601-3.

Gao, L., Loveless, J., Shay, C., Teng, Y., 2020. Targeting ROS-mediated crosstalk between autophagy and apoptosis in cancer. Adv. Exp. Med. Biol. 1260, 1–12. https://doi.org/10.1007/978-3-030-42667-5_1.

Gattone, V.H. 2nd, Wang, X., Harris, P.C., Torres, V.E., 2003. Inhibition of renal cystic disease development and progression by a vasopressin V2 receptor antagonist. Nat. Med. 9, 1323–1326. https://doi.org/10.1038/nm935.

Greenberg, A., Verbalis, J.G., Amin, A.N., Burst, V.R., Chiodo 3rd, J.A., Chiong, J.R., Dasta, J.F., Friend, K.E., Hauptman, P.J., Peri, A., Sigal, S.H., 2015. Current treatment practice and outcomes. Report of the hyponatremia registry. Kidney Int. 88, 167–177. https://doi.org/10.1038/ki.2015.4.

Grohé, C., 2019. Hyponatremia in Oncology patients. Front. Horm. Res. 52, 161–166. https://doi.org/10.1159/000493245.

Hansen, O., Sørensen, P., Hansen, K.H., 2010. The occurrence of hyponatremia in SCLC and the influence on prognosis: a retrospective study of 453 patients treated in a single institution in a 10-year period. Lung Canc. 68, 111–114. https://doi.org/10.1016/j.lungcan.2009.05.015.

Hemmati, M., Yousefi, B., Bahar, A., Eslami, M., 2021. Importance of heme oxygenase-1 in gastrointestinal cancers: functions, inductions, regulations, and signaling. J. Gastrointest. Canc. https://doi.org/10.1007/s12029-021-00587-0.

Holland-Bill, L., Christiansen, C.F., Heide-Jørgensen, U., Ulrichsen, S.P., Ring, T., Jørgensen, J.O.L., Sørensen, H.T., 2015. Hyponatremia and mortality risk: a Danish cohort study of 279 508 acutely hospitalized patients. Eur. J. Endocrinol. 173, 71–81. https://doi.org/10.1530/EJE-15-0111.

Jeppesen, A.N., Jensen, H.K., Donskov, F., Marcussen, N., von der Maase, H., 2010. Hyponatremia as a prognostic and predictive factor in metastatic renal cell carcinoma. Br. J. Canc. 102, 867–872. https://doi.org/10.1038/sj.bjc.6605563.

Kakiuchi, M., Nishizawa, T., Ueda, H., Gotoh, K., Tanaka, A., Hayashi, A., Yamamoto, S., Tatsuno, K., Katoh, H., Watanabe, Y., Ichimura, T., Ushiku, T., Funahashi, S., Tateishi, K., Wada, I., Shimizu, N., Nomura, S., Koike, K., Seto, Y., Fukayama, M., Aburatani, H., Ishikawa, S., 2014. Recurrent gain-of-function mutations of RHOA in diffuse-type gastric carcinoma. Nat. Genet. 46, 583–587. https://doi.org/10.1038/ng.2984.

Kasi, P.M., 2012. Proposing the use of hyponatremia as a marker to help identify high risk individuals for lung cancer. Med. Hypotheses 79, 327–328. https://doi.org/10.1016/j.mehy.2012.05.023.

Kim, H.S., Yi, S.Y., Jun, H.J., Lee, J., Park, J.O., Park, Y.S., Jang, J., Kim, H.-J., Ko, Y., Lim, H.Y., Kang, W.K., 2007. Clinical outcome of gastric cancer patients with bone marrow metastases. Oncology 73, 192–197. https://doi.org/10.1159/000127386.

Kobayashi, N., Usui, S., Yamaoka, M., Suzuki, H., Kikuchi, S., Goto, Y., Sakai, M., Sato, Y., 2014. The influence of serum sodium concentration on prognosis in resected non-small cell lung cancer. Thorac. Cardiovasc. Surg. 62, 338–343. https://doi.org/10.1055/s-0033-1359713.

Marroncini, G., Fibbi, B., Errico, A., Grappone, C., Maggi, M., Peri, A., 2020. Effects of low extracellular sodium on proliferation and invasive activity of cancer cells in vitro. Endocrine 67, 473–484. https://doi.org/10.1007/s12020-019-02135-0.

Moore, S.M., Rintoul, R.C., Walker, T.R., Chilvers, E.R., Haslett, C., Sethi, T., 1998. The presence of a constitutively active phosphoinositide 3-kinase in small cell lung cancer cells mediates anchorage-independent proliferation via a protein kinase B and p70(s6k)-dependent pathway. Canc. Res. 58, 5239–5247.

Oronsky, B., Caroen, S., Oronsky, A., Dobalian, V.E., Oronsky, N., Lybeck, M., Reid, T.R., Carter, C.A., 2017. Electrolyte disorders with platinum-based chemotherapy: mechanisms, manifestations and management. Canc. Chemother. Pharmacol. 80, 895–907. https://doi.org/10.1007/s00280-017-3392-8.

Pérez-Ramírez, C., Cañadas-Garre, M., Molina, M.Á., Faus-Dáder, M.J., Calleja-Hernández, M.Á., 2015. PTEN and PI3K/AKT in non-small-cell lung cancer. Pharmacogenomics 16, 1843–1862. https://doi.org/10.2217/pgs.15.122.

Peri, A., 2013. Clinical review: the use of vaptans in clinical endocrinology. J. Clin. Endocrinol. Metab. 98, 1321–1332. https://doi.org/10.1210/jc.2012-4082.

Petereit, C., Zaba, O., Teber, I., Grohé, C., 2011. [Is hyponatremia a prognostic marker of survival for lung cancer?]. Pneumologie 65, 565–571. https://doi.org/10.1055/s-0030-1256668.

Petereit, C., Zaba, O., Teber, I., Lüders, H., Grohé, C., 2013. A rapid and efficient way to manage hyponatremia in patients with SIADH and small cell lung cancer: treatment with tolvaptan. BMC Pulm. Med. 13, 55. https://doi.org/10.1186/1471-2466-13-55.

Sakata-Yanagimoto, M., Enami, T., Yoshida, K., Shiraishi, Y., Ishii, R., Miyake, Y., Muto, H., Tsuyama, N., Sato-Otsubo, A., Okuno, Y., Sakata, S., Kamada, Y., Nakamoto-Matsubara, R., Tran, N.B., Izutsu, K., Sato, Yusuke, Ohta, Y., Furuta, J., Shimizu, S., Komeno, T., Sato, Yuji, Ito, T., Noguchi, M., Noguchi, E., Sanada, M., Chiba, K., Tanaka, H., Suzukawa, K., Nanmoku, T., Hasegawa, Y., Nureki, O., Miyano, S., Nakamura, N., Takeuchi, K., Ogawa, S., Chiba, S., 2014. Somatic RHOA mutation in angioimmunoblastic T cell lymphoma. Nat. Genet. 46, 171–175. https://doi.org/10.1038/ng.2872.

Schrier, R.W., Gross, P., Gheorghiade, M., Berl, T., Verbalis, J.G., Czerwiec, F.S., Orlandi, C., 2006. Tolvaptan, a selective oral vasopressin V2-receptor antagonist, for hyponatremia. N. Engl. J. Med. 355, 2099–2112. https://doi.org/10.1056/NEJMoa065181.

Sengupta, A., Banerjee, S.N., Biswas, N.M., Jash, D., Saha, K., Maji, A., Bandyopadhyaya, A., Agarwal, S., 2013. The incidence of hyponatraemia and its effect on the ECOG performance status among lung cancer patients. J. Clin. Diagn. Res. 7, 1678–1682. https://doi.org/10.7860/JCDR/2013/5900.3225.

Shi, J., Surma, M., Zhang, L., Wei, L., 2013. Dissecting the roles of ROCK isoforms in stress-induced cell detachment. Cell Cycle 12, 1492–1500. https://doi.org/10.4161/cc.24699.

Shoaf, S.E., Kim, S.R., Bricmont, P., Mallikaarjun, S., 2012. Pharmacokinetics and pharmacodynamics of single-dose oral tolvaptan in fasted and non-fasted states in healthy Caucasian and Japanese male subjects. Eur. J. Clin. Pharmacol. 68, 1595–1603. https://doi.org/10.1007/s00228-012-1295-5.

Sinha, S., Dwivedi, N., Tao, S., Jamadar, A., Kakade, V.R., Neil, M.O., Weiss, R.H., Enders, J., Calvet, J.P., Thomas, S.M., Rao, R., 2020. Targeting the vasopressin type-2 receptor for renal cell carcinoma therapy. Oncogene 39, 1231–1245. https://doi.org/10.1038/s41388-019-1059-0.

Sørensen, J.B., Andersen, M.K., Hansen, H.H., 1995. Syndrome of inappropriate secretion of antidiuretic hormone (SIADH) in malignant disease. J. Intern. Med. 238, 97–110. https://doi.org/10.1111/j.1365-2796.1995.tb00907.x.

Tanaka, K., Takeda, S., Mitsuoka, K., Oda, T., Kimura-Sakiyama, C., Maéda, Y., Narita, A., 2018. Structural basis for cofilin binding and actin filament disassembly. Nat. Commun. 9, 1860. https://doi.org/10.1038/s41467-018-04290-w.

Tiseo, M., Buti, S., Boni, L., Mattioni, R., Ardizzoni, A., 2014. Prognostic role of hyponatremia in 564 small cell lung cancer patients treated with topotecan. Lung Canc. 86, 91–95. https://doi.org/10.1016/j.lungcan.2014.07.022.

Torres, V.E., Chapman, A.B., Devuyst, O., Gansevoort, R.T., Grantham, J.J., Higashihara, E., Perrone, R.D., Krasa, H.B., Ouyang, J., Czerwiec, F.S., 2012. Tolvaptan in patients with autosomal dominant polycystic kidney disease. N. Engl. J. Med. 367, 2407–2418. https://doi.org/10.1056/NEJMoa1205511.

Torres, V.E., Chapman, A.B., Devuyst, O., Gansevoort, R.T., Perrone, R.D., Koch, G., Ouyang, J., McQuade, R.D., Blais, J.D., Czerwiec, F.S., Sergeyeva, O., 2017. Tolvaptan in later-stage autosomal dominant polycystic kidney disease. N. Engl. J. Med. 377, 1930–1942. https://doi.org/10.1056/NEJMoa1710030.

Torres, V.E., Wang, X., Qian, Q., Somlo, S., Harris, P.C., Gattone, V.H. 2nd, 2004. Effective treatment of an orthologous model of autosomal dominant polycystic kidney disease. Nat. Med. 10, 363–364. https://doi.org/10.1038/nm1004.

Wald, R., Jaber, B.L., Price, L.L., Upadhyay, A., Madias, N.E., 2010. Impact of hospital-associated hyponatremia on selected outcomes. Arch. Intern. Med. 170, 294–302. https://doi.org/10.1001/archinternmed.2009.513.

Wanchoo, R., Karam, S., Uppal, N.N., Barta, V.S., Deray, G., Devoe, C., Launay-Vacher, V., Jhaveri, K.D., 2017. Adverse renal effects of immune checkpoint inhibitors: a narrative review. Am. J. Nephrol. 45, 160–169. https://doi.org/10.1159/000455014.

Wang, J., Biju, M.P., Wang, M.-H., Haase, V.H., Dong, Z., 2006. Cytoprotective effects of hypoxia against cisplatin-induced tubular cell apoptosis: involvement of mitochondrial inhibition and p53 suppression. J. Am. Soc. Nephrol. 17, 1875–1885. https://doi.org/10.1681/ASN.2005121371.

Wu, R., Li, C., Wang, Z., Fan, H., Song, Y., Liu, H., 2020. A narrative review of progress in diagnosis and treatment of small cell lung cancer patients with hyponatremia. Transl. Lung Cancer Res. 9, 2469–2478. https://doi.org/10.21037/tlcr-20-1147.

Wu, Y., Beland, F.A., Chen, S., Liu, F., Guo, L., Fang, J.-L., 2015. Mechanisms of tolvaptan-induced toxicity in HepG2 cells. Biochem. Pharmacol. 95, 324–336. https://doi.org/10.1016/j.bcp.2015.03.015.

Zinda, M.J., Johnson, M.A., Paul, J.D., Horn, C., Konicek, B.W., Lu, Z.H., Sandusky, G., Thomas, J.E., Neubauer, B.L., Lai, M.T., Graff, J.R., 2001. AKT-1, -2, and -3 are expressed in both normal and tumor tissues of the lung, breast, prostate, and colon. Clin. Canc. Res. 7, 2475–2479.